Brain stimulation and brain lesions converge on common causal circuits in neuropsychiatric disease

Supplementary Methods

Localization of lesions and stimulation sites

Localization was conducted using the following approaches:

1. Lesions were localized using head CT or brain MRI. Each lesion was manually traced and registered to common atlas space as described in prior lesion network mapping work[1].
2. DBS sites were localized on post-operative CT scans. The DBS-induced electric field was modeled using LEAD-DBS as described in prior work[2].
3. TMS sites were localized using three different approaches as described in prior work using the same datasets. In the Boston[3] and Monash[4] cohorts, patients received traditional clinical targeting using scalp landmarks, and the incidental stimulation sites were localized retrospectively using neuronavigation. In the Ann Arbor cohort[5], stimulation sites were identified using task fMRI and treatment was delivered prospectively with neuronavigation. In the OPT-TMS cohort[6], patients received scalp landmark-based targeting and the incidental stimulation sites were recorded using fiducial markers during an MRI scan. The TMS-induced electric field was modeled using a previously-validated conical model of spatial field decay[7].

Statistical methods

Unless otherwise specified, statistical analyses were conducted using permutation testing. The parameter of interest was re-computed 25,000 times after randomly re-assigning each subject's neuroimaging data to a different subject's clinical data. The resulting p-value was defined as the percentage of randomly-permuted results that were stronger than the real result. If the real result was stronger than 95% of permuted results, the result was considered significant ($p<0.05$).

Pearson's *r* was used as the primary outcome for all regression analyses. Prior to further analysis, all r-values were transformed using Fisher's r-to-z transform.

Except as otherwise specified, all quantitative analyses were conducted using MATLAB R2018b (Mathworks, Natick, MA). Additional tools were also used for data visualization. Heatmaps were constructed using Graphpad Prism 8.2.1. Box plots and scatter plots were constructed in JMP Pro 14. Brain images were visualized using Surfice (average surface space) or Connectome Workbench (subject-specific surface space).

Supplementary Results

Modality	Dataset identifier	Institution of data collection and ethics approval	Setting	*n*	Primary Outcome	Patient population	Localization approach	Age, mean (SD)	Sex
DBS (ANT)	Maastricht	Maastricht University Medical Center	Naturalistic	25	BDI	Epilepsy	Post-op CT	39 (12)	76% M, 24% F
DBS (STN)	Berlin	Charite University Medicine Berlin	Naturalistic	32	BDI	Parkinson disease	Post-op CT	61 (10)	69% M, 31% F
DBS (VC/VS)	Boston	Massachusetts General Hospital	Clinical trial	8	MADRS	MDD	Post-op CT	40 (17)	62% M, 38% F
DBS (sgACC)	Berlin	Charite University Medicine Berlin	Clinical trial	9	HAMD	MDD	Post-op CT	45 (10)	33% M, 67% F
DBS (sgACC)	Atlanta	Emory University Hospital	Clinical trial	27	HAMD	MDD	Post-op CT	50 (13)	56% M, 44% F
TMS ("5.5 cm rule")	Boston	Beth Israel Deaconess Medical Center	Naturalistic	30	BDI	MDD	Retrospective Neuronavigation	53 (10)	33% M, 67% F
TMS (Beam F3)	Monash	Epworth Healthcare, Monash University	Naturalistic	24	BDI	MDD	Retrospective Neuronavigation	44 (13)	50% M, 50% F
TMS (Task fMRI)	Ann Arbor	University of Michigan Hospital	Clinical trial	16	MADRS	MDD	Prospective Neuronavigation	47 (11)	69% F, 31% M
TMS ("5 cm rule")	OPT-TMS	MUSC, NYPH, Emory, UW*	Multi-center trial	81	HAMD	MDD	MRI fiducial marker	47 (11)	57% F, 43% M
Lesions (penetrating)	VHIS	US Army Medical Research Command	Observational	196	BDI	Penetrating TBI	CT (chronic)	58 (3)	100% M
Lesions (stroke)	St. Louis	Barnes-Jewish Hospital, Washington Unviersity	Observational	100	GDS	Ischemic stroke	MRI	54 (11)	51% M, 49% F
Lesions (stroke)	Melbourne	Austin Hospital, Box Hill Hospital, Royal Melbourne Hospital	Observational	63	PHQ9	Ischemic stroke	MRI	67 (13)	65% M, 35% F
Lesions (stroke)	Monash	Southern Health, Monash University	Observational	55	HADS	Ischemic stroke	MRI	63 (14)	61% M, 39% F
Lesions (stroke)	Chicago	Northwestern Memorial Hospital	Observational	51	SF36	Hemorrhagic stroke	CT (acute)	61 (14)	55% M, 45% F

Supplementary Table 1: 14 datasets were included in this analysis across various stimulation sites, study settings, sample sizes, outcome metrics, patient populations, and localization approaches. To address heterogeneity in depression scales and other methods, each dataset was analyzed independently. The modalities were classified into three categories, including DBS, TMS, and lesions. DBS targets included anterior nucleus of the thalamus (ANT), subthalamic nucleus (STN), ventral capsule/ventral striatum (VC/VS), and subgenual anterior cingulate cortex (sgACC). TMS targets were within different parts of the dorsolateral prefrontal cortex, including 5 cm or 5.5 cm anterior to the motor cortex ("5 cm rule" or "5.5 cm rule"), a scalp measurement technique that estimates the location of the EEG F3 electrode (Beam F3), and a task fMRI-based target. Lesions included penetrating head trauma, ischemic stroke, and hemorrhagic stroke.

*Medical Univeristy of South Carolina, New York Presbyterian Hospital (Columbia University), Emory University Hospital, and University of Washington Medical Center.

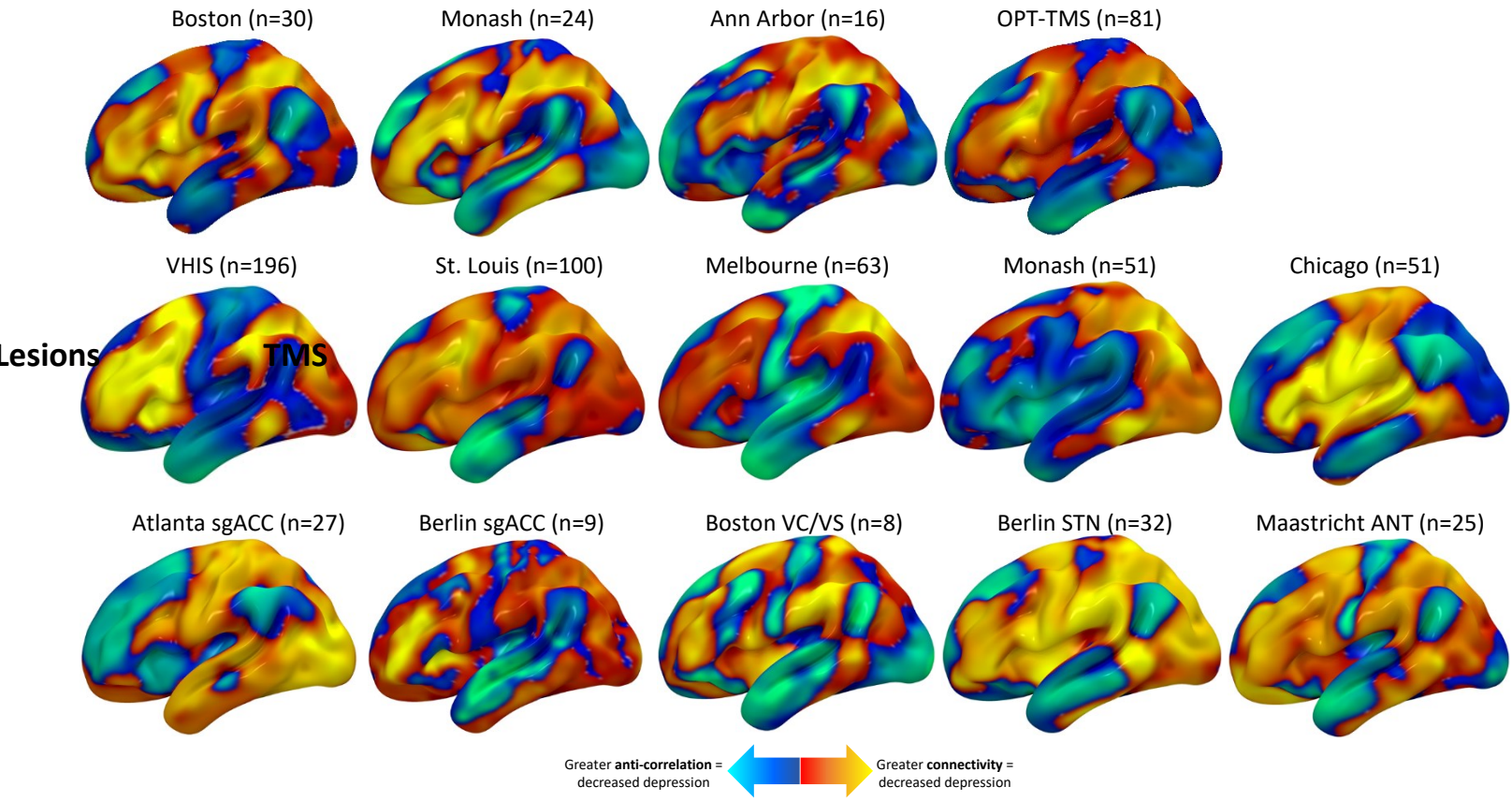

Supplementary Figure 1: Circuit maps generated from each of the 14 datasets.

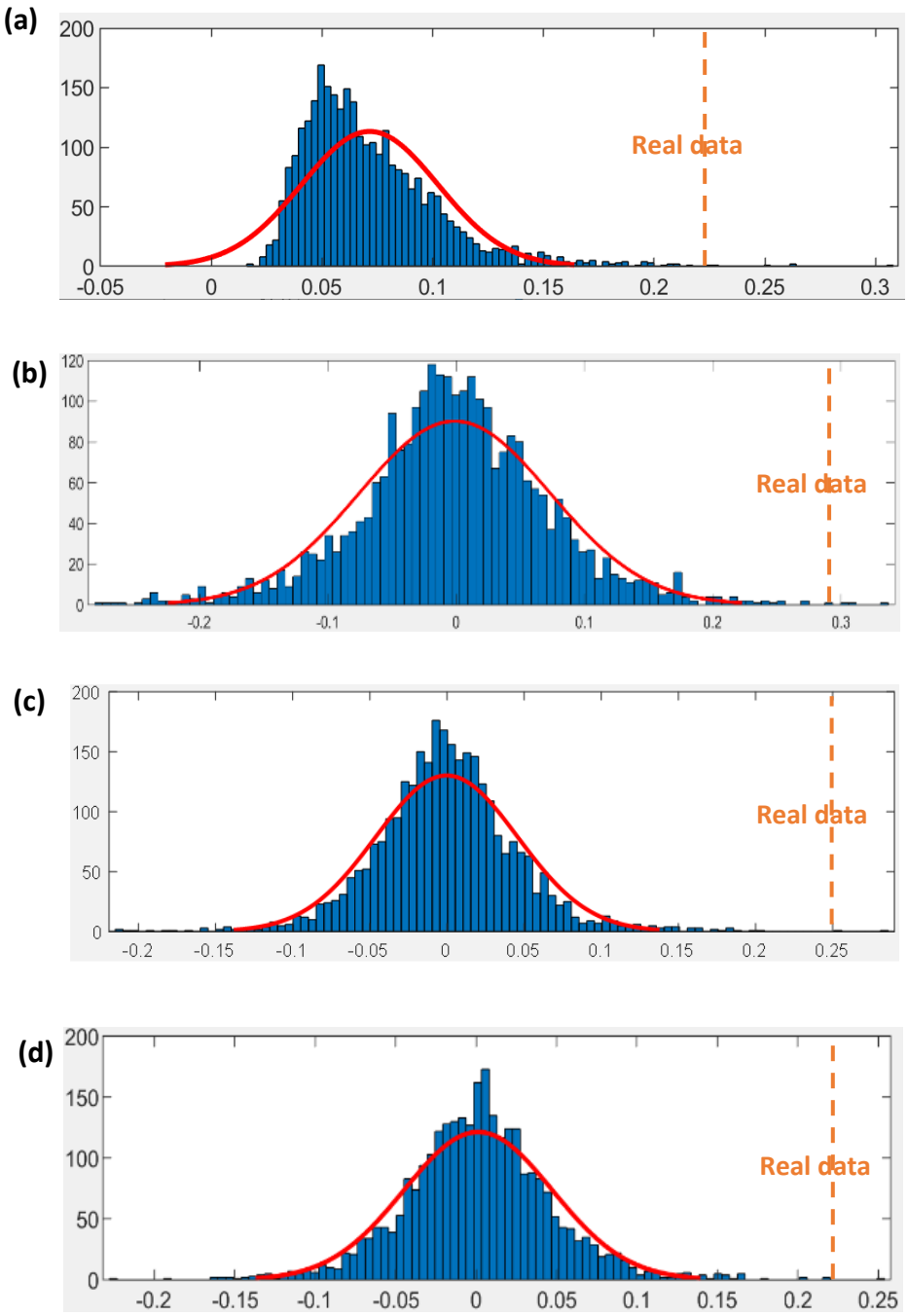

Supplementary Figure 2: Permutation test confirmed that the cross-cohort spatial correlations were stronger than expected by the chance distribution. **(a)** Mean spatial correlation between all fourteen datasets in comparison with the chance distribution. **(b)** Mean spatial correlation between TMS, DBS, and lesion datasets (categorized by modality) in comparison with the chance distribution. **(c)** Mean spatial correlation between MDD and non-MDD datasets in comparison with the chance distribution. **(d)** Mean spatial correlation between lesion and neuromodulation datasets in comparison

Positive peaks:

Region	Coordinates	Cluster size (mm^3)	t-value
Left dorsolateral prefrontal cortex	(-53, 41, 15)	152	4.29
Right dorsolateral prefrontal cortex	(48, 38, 23)	1128	4.79
Left inferior frontal gyrus	(-46, 9, 31)	6024	4.93
Right inferior frontal gyrus	(46, 4, 35)	2112	4.74
Left intraparietal sulcus	(-33, -53, 46)	8384	5.00
Right intraparietal sulcus	(34, -51, 46)	8152	4.91
Left extrastriate visual cortex	(-57, -50, -8)	264	4.52

Negative peaks:

Region	Coordinates	Cluster size (mm^3)	t-value
Subgenual cingulate cortex	(8, 24, -4)	1136	-4.66
Ventromedial prefrontal cortex	(-6, 58, 10)	1144	-4.46

Supplementary Table 2: Positive and negative peaks in the combined circuit map.

(a) **(b)**

Supplementary Figure 3: Specificity to depression versus other emotional/cognitive symptoms. (a) Our leave-one-dataset-out depression circuit (n=517) was more correlated with the VHIS depression circuit (n=196) than any other VHIS symptom circuit. **(b)** Our leave-one-dataset-out depression circuit (n=613) was more correlated with the St. Louis depression circuit (n=100) than any other St. Louis cognitive circuit.

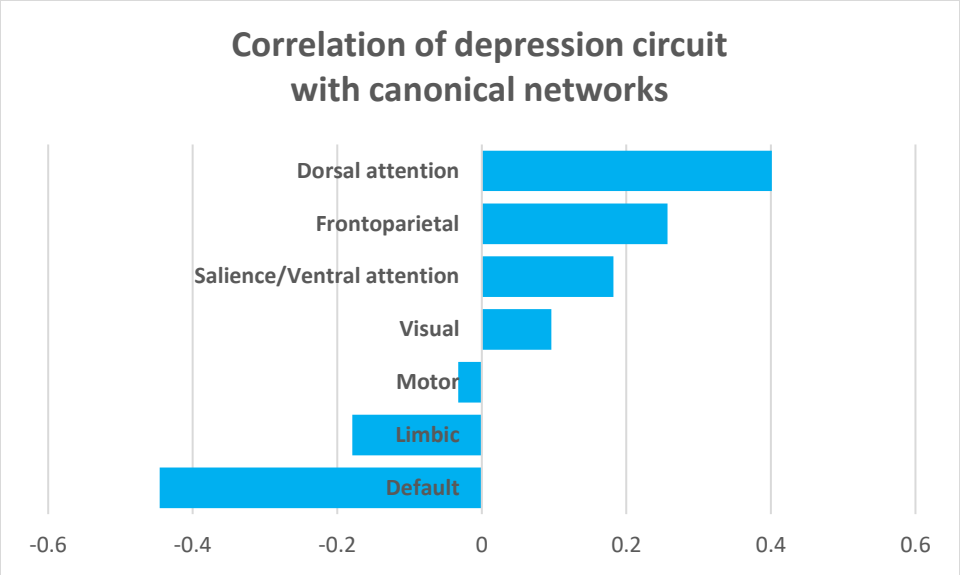

Supplementary Figure 4: In comparison with the canonical 7-network parcellation by Yeo et al.[8], our depression circuit was most similar to the dorsal attention and frontoparietal control networks, and was most anti-correlated with the default mode and limbic networks.

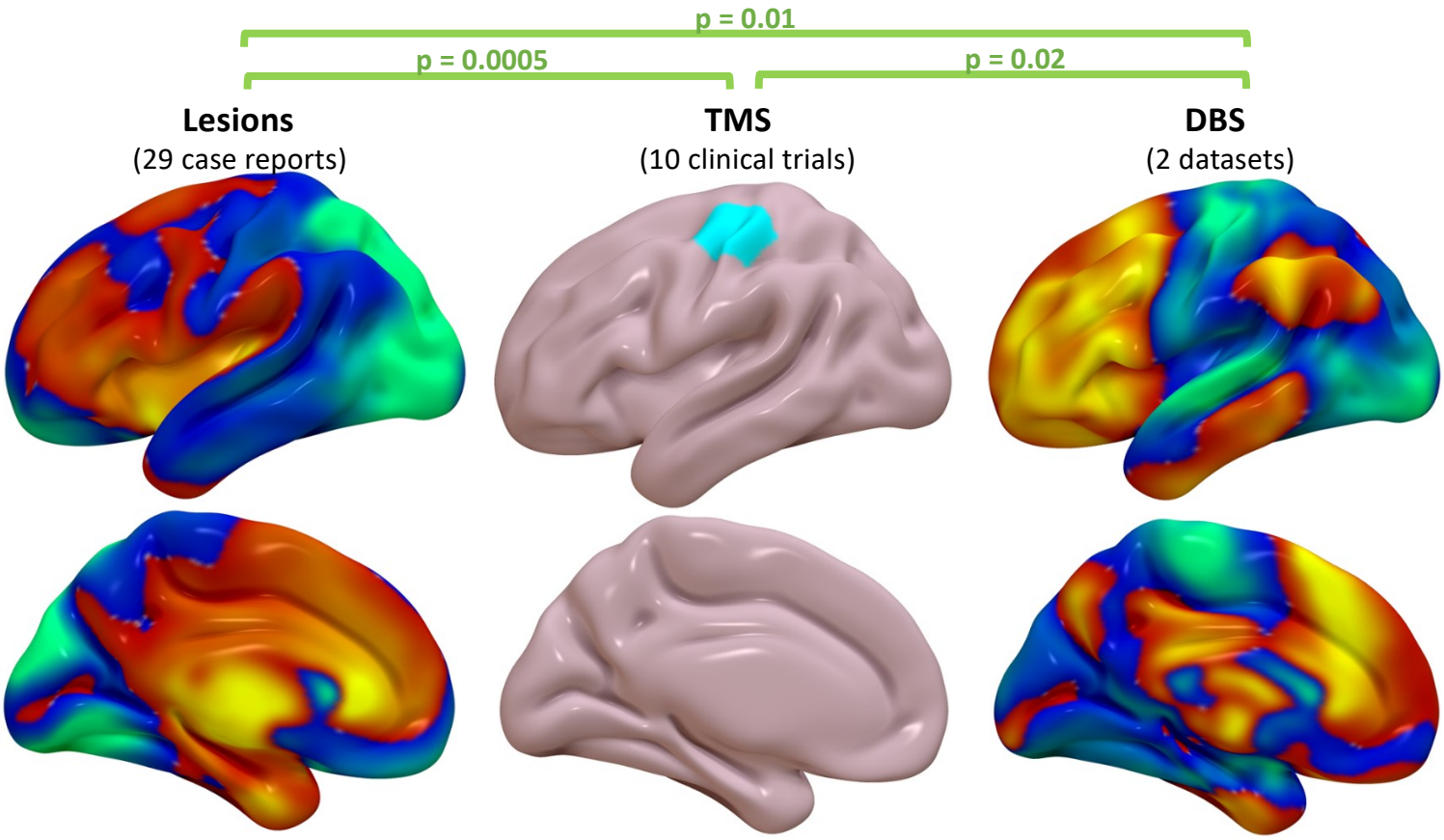

Supplementary Figure 5: Lesion/stimulation site network mapping also predicts optimal treatment targets for Parkinson disease (PD). PD circuit maps were significantly similar between lesion datasets and DBS datasets. Both of these maps predicted that primary motor cortex would be an effective TMS site, consistent with a recent meta-analysis of 10 clinical trials[9]. For display purposes, PD circuit maps were averaged (weighted mean) across datasets within each modality.

Supplementary references

1. Padmanabhan JL, Cooke D, Joutsa J, et al. A human depression circuit derived from focal brain lesions. *Biological Psychiatry.* 2019.
2. Horn A, Reich M, Vorwerk J, et al. Connectivity Predicts deep brain stimulation outcome in Parkinson disease. *Ann Neurol.* 2017;82(1):67-78.
3. Weigand A, Horn A, Caballero R, et al. Prospective Validation That Subgenual Connectivity Predicts Antidepressant Efficacy of Transcranial Magnetic Stimulation Sites. *Biol Psychiatry.* 2018;84(1):28-37.
4. Cash RFH, Zalesky A, Thomson RH, Tian Y, Cocchi L, Fitzgerald PB. Subgenual Functional Connectivity Predicts Antidepressant Treatment Response to Transcranial Magnetic Stimulation: Independent Validation and Evaluation of Personalization. *Biol Psychiatry.* 2019;86(2):e5-e7.
5. Taylor SF, Ho SS, Abagis T, et al. Changes in brain connectivity during a sham-controlled, transcranial magnetic stimulation trial for depression. *J Affect Disord.* 2018;232:143-151.
6. Johnson KA, Baig M, Ramsey D, et al. Prefrontal rTMS for treating depression: location and intensity results from the OPT-TMS multi-site clinical trial. *Brain Stimul.* 2013;6(2):108-117.
7. Fox MD, Liu H, Pascual-Leone A. Identification of reproducible individualized targets for treatment of depression with TMS based on intrinsic connectivity. *Neuroimage.* 2013;66:151-160.
8. Yeo BT, Krienen FM, Sepulcre J, et al. The organization of the human cerebral cortex estimated by intrinsic functional connectivity. *J Neurophysiol.* 2011;106(3):1125-1165.
9. Yang C, Guo Z, Peng H, et al. Repetitive transcranial magnetic stimulation therapy for motor recovery in Parkinson's disease: A Meta-analysis. *Brain Behav.* 2018;8(11):e01132.